Journal of Solid State Chemistry **149,** 428–433 (2000)
doi:10.1006/jssc.1999.8575, available online at http://www.idealibrary.com on IDEAL®

Superstructure and Twinning in the Tetragonal Tungsten Bronze-Type Phase $Nb_7W_{10}O_{47}$

Frank Krumeich,*,[1] Michael Wörle,* and Altaf Hussain†

** Laboratory of Inorganic Chemistry, ETH Zürich, CH-8092 Zürich, Switzerland; and †Department of Chemistry, University of Dhaka, Dhaka 1000, Bangladesh*

Received July 1, 1999; in revised form October 14, 1999; accepted November 5, 1999

DEDICATED TO PROFESSOR REGINALD GRUEHN ON THE OCCASION OF HIS 70TH BIRTHDAY

Needle-shaped crystals of $Nb_7W_{10}O_{47}$, a member of the solid solution series $Nb_{8-n}W_{9+n}O_{47}$ with $n = 1$, were prepared from the binary oxides with $HgCl_2$ added as a mineralizer. All investigated crystals were twinned. The data set was measured on a fourling, which consists of 73% of an individual twin domain. The orthorhombic structure ($a = 1225.7(2)$, $b = 3663.3(6)$, $c = 394.96(6)$ pm) was refined in the space group $P2_12_12$ (No. 18) to a final R value of 5.11%. The composition of this crystal determined from X-ray data is $Nb_{6.7}W_{10.3}O_{47}$. $Nb_7W_{10}O_{47}$ crystallizes isostructural to $Nb_8W_9O_{47}$ in a threefold superstructure of the tetragonal tungsten bronze type. All atomic positions are considerably shifted out of the planes (001) and (002), leading to alternating short (~ 175 pm) and long (~ 220 pm) metal–oxygen distances along the short crystallographic c axis. One octahedral site is exclusively occupied by W, the center of the pentagonal bipyramid preferentially by Nb.

1. INTRODUCTION

$Nb_8W_9O_{47}$ (1), which crystallizes in a threefold superstructure of the tetragonal tungsten bronze (TTB) type (2), represents not only a very stable phase in the pseudobinary system Nb_2O_5/WO_3 (3, 4), but this structure is also favored in other systems if the metal/oxygen ratio is 17:47. Several isostructural niobium tungsten oxides are accessible by a (formal) substitution of Nb^{5+} according to $2Nb^{5+} = M^{4+} + W^{6+}$: solid solution series $M_n^{4+}Nb_{8-2n}W_{9+n}O_{47}$ with mixed oxidation states prepared with $M = Nb$ ($0 \le n \le 4$) and W ($0 \le n \le 2.5$) (5); the quaternary phases $MNb_6W_{10}O_{47}$ with $M = Ti$, Zr, and Hf and $M_2Nb_4W_{11}O_{47}$ with $M = Ti$ and Hf (6). The high-temperature form of $Ta_8W_9O_{47}$ also crystallizes in this structure (1, 7).[2] Furthermore, disordered variants of the $Nb_8W_9O_{47}$ structure were found by high-resolution transmission electron microscopy (HRTEM) in the quarternary system Na/Nb/W/O, e.g. for the composition $Na_{0.2}Nb_{4.2}W_{1.8}O_{16}$ (9), and for the potassium niobium oxide fluoride $K_3Nb_{12}O_{31}F$ (10), which represents the only tungsten-free example of this structure type uncovered until now.

The TTB structure consists of a framework of corner-sharing octahedra, with tunnels of trigonal, square, and pentagonal shape running along the short crystallographic c axis. The superstructure of $Nb_8W_9O_{47}$ ($a_{TTB} \times 3a_{TTB} \times c_{TTB}$) is caused by filling one third of the pentagonal tunnels with metal–oxygen strings in a systematic way (1). The resulting MO_7 pentagonal pyramid (M = Nb, W) in connection with the five adjacent MO_6 octahedra build up the structural element designated as a pentagonal column (11, 12).

Detailed HRTEM studies have revealed a lot of information about the real structure of these phases (5–7, 13–15). Twinning (twinning plane: (130)) and fault boundaries, which cause a displacement of $1/3b$ between the unit cells in adjacent domains, appear frequently. The disorder caused by these microstructural features has rendered X-ray single-crystal structure determinations on these phases difficult, and structure models based on single-crystal data have been established for $Nb_8W_9O_{47}$ only. Sleight (1) as well as Craig and Stephenson (16)[3] derived approximate models using the reflections $hk0$ only. As a result, all atoms are located on the planes (001) and (002) which therefore become mirror planes. This symmetry element is not present in the noncentrosymmetric space group $P2_12_12$. In order to enlighten this contradiction, we redetermined this structure using all reflections hkl collected from a twinned crystal, which had been selected from a sample of composition $Nb_7W_{10}O_{47}$.

[1] To whom correspondence should be addressed. E-mail: krumeich@solid.phys.ethz.ch.

[2] It is noteworthy that $Nb_8W_9O_{47}$ and $Ta_8W_9O_{47}$ can be used as matrix structures for the reversible electrochemical insertion of lithium (8).

[3] The authors of the latter paper determined the structure from a twinned crystal and discussed a wrong ninefold TTB superstructure ($3a_{TTB} \times 3a_{TTB} \times c_{TTB}$) besides the threefold superstructure. However, the main features of the stucture as well as the atomic positions are very similar to Sleight's model. They did not calculate the Nb/W occupancy factors.

0022-4596/00 $35.00

2. EXPERIMENTAL

Preparation

The binary oxides Nb_2O_5, WO_3 (both puriss., Fluka AG), and NbO_2 (prepared by reduction of Nb_2O_5 with Niobium foil) were mixed in the molar ratio 3:10:1, giving the composition $Nb_7W_{10}O_{47}$. This mixture was heated together with about 4 mg $HgCl_2$ (mineralizer) in an evacuated silica tube for 3 days at 1250°C (5). The product consists of dark blue, needle-shaped crystals with a metallic lustre. The X-ray powder diffraction data are given in (5).

Data Collection and Structure Determination

Several crystals were tested on a Siemens SMART platform diffractometer equipped with a CCD detector, and a crystal was selected which showed the reflections of the threefold TTB superstructure mainly in only one direction of the substructure. A data set covering a whole sphere up to $2\Theta = 80°$ was collected (7200 frames, step width 0.3° in ω, exposure time 20 s per frame). The data were integrated with the SAINT program (17) and corrected for Lorentz factor, polarization, air absorption, and absorption due to the path length through the detector faceplate. The final cell constants were refined from 8472 reflections and corrected for systematic deviations which had been determined from a reference measurement with a ruby sphere. The structure was refined by means of the program SHELXTL (18). Details of the data collection and structure refinement procedure are given in Table 1.

TABLE 1
Crystal Data and Structure Refinement for $Nb_7W_{10}O_{47}$

Empirical formula	$Nb_{6.70(6)}W_{10.30(4)}O_{47}$
Formula weight	3268.15
Temperature	293(2) K
Wavelength	71.073 pm
Crystal system	orthorhombic
Space group	$P2_12_12$ (No. 18)
Unit cell dimensions	$a = 1225.67(18)$ pm
	$b = 3663.3(6)$ pm
	$c = 394.96(6)$ pm
Volume	1.7734(5) nm^3
Z	2
Density (calculated)	6.120 mg/m^3
Absorption coefficient	35.458 mm^{-1}
$F(000)$	2826
Crystal size	$0.12 \times 0.12 \times 0.54$ mm^3
Θ range for data collection	$1.11 \le \Theta \le 40.14°$.
Index ranges	$-22 \le h \le 22$,
	$-66 \le k \le 66$,
	$-6 \le l \le 6$
Reflections collected	50599
Independent reflections	10732 [R(int) = 0.0722]
Completeness to $\Theta = 40.14°$	97.0%
Max. and min. transmission	0.13687 and 0.01329
Refinement method	Full-matrix least-squares on F^2
Data/restraints/parameters	50599/2/184
Goodness-of-fit on F^2	1.003
Final R indices [$I > 2\sigma(I)$]	$R1 = 0.0511$, w$R2 = 0.1213$
R indices (all data)	$R1 = 0.0630$, w$R2 = 0.1257$
Absolute structure parameter	0.000(11)
Extinction coefficient	0.000631(17)
Largest difference peak and hole	4.402 and -4.028 e × $Å^{-3}$

All metal atom positions (Table 2) were found by direct methods (18). The oxygen atom positions were detected in the difference Fourier map after applying the following twin laws. The observed twinning can be described by a rotation of 90° around the crystallographic c axis, and, in addition, the inversion twins of the main and the rotated individuum are present, leading to a fourling. The main individuum and the rotated component were refined as free parameters to values of 0.727(37) and 0.069(14) of the total volume. The volumes of the inversion twins are present with fractions of 0.087(9) and 0.117(14), respectively.

Several weak reflections at low diffraction angles violate the extinction rules for the 2_1 screw axes along the crystallographic a and b axes. Measurements on a four-circle diffractometer showed for the strongest of the violations that they can be attributed either to multiple diffraction or to the $\lambda/2$ effect. Neglecting these reflections, the space group $P2_12_12$ is unambiguously determined.

Due to the needle-like shape of the crystals and the very high linear absorption coefficient of 35.45 mm^{-1}, special attention had to be given to the absorption. An empirical absorption correction (19) did not lead to satisfying results, since especially the absorption along the needle axis could not be corrected properly. On the other hand, a reliable determination of the crystal faces other than {001} turned out to be difficult. Therefore, a numerical absorption correction was performed after a refinement of the distances of all faces $hk0$ by minimizing $R_{int.}$ (18, 20). The internal R value, calculated for the Laue symmetry mmm (6211 unique reflections), was 0.203 before and 0.077 after correction.

Two metal atom positions (Nb, W)2 and (Nb, W)4 had to be described as split positions (see Table 2 and Fig. 3) with a strongly preferred occupation of one site. The metal atoms except the splitted sites (Nb, W)2*A*, Nb2*B*, (Nb, W)4*A*, and Nb4*B* were refined with anisotropic displacement parameters (Table 3).

The anisotropic refinement for the oxygen atoms was not possible. Since the metal–oxygen distance is dependent on the sort of the metal atoms and all metal atom sites except W6 are occupied in a statistical way by Nb and W atoms, the oxygen atom positions are expected to adapt to the local surroundings with specific metal atoms, leading to disorder in the oxygen sublattice as well. Moreover, it is a well-known problem to locate atoms with very few electrons in the neighborhood of strongly diffracting atoms like tungsten and/or niobium.

TABLE 2
Atomic Coordinates ($\times 10^4$) and Equivalent Isotropic Displacement Parameters U(eq) (Å$\times 10^4$) and Site Occupation (in %)

Atom	x	y	z	U_{eq}	Occupation
(Nb, W)(1)	0	5000	5648(1)	78(1)	23.1(3), 76.9(3)
(Nb, W)(2*A*)	4251(1)	4298(1)	4394(2)	57(1)	38.6(4), 49.2(2)
Nb(2*B*)	4240(3)	4304(1)	5605(18)	57(1)	12.2(3)
(Nb, W)(3)	9294(1)	4028(1)	4263(1)	51(1)	29.4(2), 70.6(2)
(Nb, W)(4*A*)	7901(1)	3067(1)	4393(2)	56(1)	14.4(4), 58.6(2)
Nb(4*B*)	7897(2)	3064(1)	5515(9)	56(1)	27.1(3)
(Nb, W)(5)	2053(1)	3610(1)	5668(1)	69(1)	43.0(2), 57.0(2)
W(6)	4844(1)	3267(1)	4171(1)	52(1)	100
(Nb, W)(7)	5793(1)	2323(1)	5577(1)	77(1)	34.6(3), 65.4(3)
(Nb, W)(8)	7066(1)	4787(1)	4371(1)	58(1)	40.8(2), 59.2(2)
(Nb, W)(9)	6685(1)	3899(1)	5580(1)	59(1)	83.5(2), 16.5(2)
O(1)	4880(3)	3286(1)	−227(11)	149(9)	100
O(2)	9246(4)	4021(1)	− 178(11)	136(9)	100
O(3)	0	5000	67(14)	144(13)	100
O(4)	7050(4)	4775(1)	− 96(11)	124(9)	100
O(5)	2052(4)	3623(1)	90(12)	176(10)	100
O(6)	5770(4)	2339(1)	42(11)	152(10)	100
O(7)	7857(4)	3094(1)	− 53(10)	126(9)	100
O(8)	4286(4)	4301(1)	− 65(11)	127(9)	100
O(9)	6693(3)	3896(1)	72(9)	80(7)	100
O(10)	2910(4)	4060(1)	4994(10)	129(9)	100
O(11)	7080(4)	2637(1)	4998(9)	93(8)	100
O(12)	7849(3)	4295(1)	4952(8)	59(7)	100
O(13)	4945(4)	2782(1)	4836(11)	103(8)	100
O(14)	5034(3)	3813(1)	4956(9)	54(7)	100
O(15)	6428(3)	3346(1)	4969(9)	74(8)	100
O(16)	6453(3)	1885(1)	4910(10)	112(9)	100
O(17)	9932(4)	4484(1)	4912(11)	146(10)	100
O(18)	584(4)	3774(1)	4969(11)	153(10)	100
O(20)	8218(3)	3625(1)	4996(9)	63(8)	100
O(21)	5887(3)	4412(1)	5062(9)	55(7)	100
O(22)	6159(4)	5200(1)	4966(10)	100(8)	100
O(23)	9315(3)	2911(1)	4926(10)	99(8)	100
O(24)	8416(4)	5003(1)	5004(10)	117(9)	100
O(25)	3395(3)	3344(1)	4928(10)	101(9)	100

Note. U_{eq} is defined as one third of the trace of the orthogonalized U^{ij} tensor.

3. RESULTS AND DISCUSSION

Microcrystalline $Nb_8W_9O_{47}$ was originally prepared by heating the binary oxides in a molar ratio $Nb_2O_5 : WO_3 = 4:9$ (1, 3). Compared to that, the crystalinity has been significantly improved by performing the reaction between the oxides in vacuum and adding $HgCl_2$ as a transporting agent. This procedure has the further advantage that also phases containing not fully oxidized cations are accessible by heating mixtures of Nb_2O_5 and WO_3 with NbO_2 or WO_2, respectively (5), e.g., leading to $Nb_7W_{10}O_{47}$.

$Nb_7W_{10}O_{47}$ crystallizes in the form of needles which are up to 2 mm long and which often are grown together (Fig. 1). This morphology points to a strongly anisotropic crystal growth. The growth direction was found to be parallel to the short crystallographic c axis. SEM micrographs (Fig. 1) show that most needles are terminated at both ends by well-developed planes {001} while their cross sections do not have clearly differentiated crystal facets. As already mentioned above, the lack of crystal planes $\{hk0\}$ that can be assigned unambiguously with indices impeded the numerical absorption correction in the course of the structure determination. This observation is in accordance with the results of TEM investigations (5), which have shown that the crystal structure of $Nb_7W_{10}O_{47}$ is disordered in the a–b plane. Occasionally, another (macroscopic) crystal fault can be detected in the SEM images (Fig. 1d): holes which are visible in the (001) plane belong to large channels running along the needle axis. The tubular morphology indicates a strongly disturbed crystal growth. Similar defects were found in phases with block structures which had been prepared via the gas phase by chemical transport reactions (21).

In fact, all crystals we investigated by X-ray diffraction were twinned, and the reflections of the threefold superstructure appear along both axes of the substructure in the a^*b^* plane. This feature had been first uncovered by electron diffraction, and structural models were derived from corresponding HTTEM images (13, 15). These models describe the arrangement of metal atoms in projection along [001]. Thus, it cannot be decided from TEM images whether a rotational twin (twin axis [001]) or a reflection twin (twinning plane {130}) is present. Furthermore, the corresponding enantiomorphs cannot be recognized since only the z parameter of the atom positions is different. On the other hand, the present X-ray structure determination shows that the selected crystal indeed comprises all four possible twin variants.

In projection along the c axis (Fig. 2), the derived structure of $Nb_7W_{10}O_{47}$ is essentially the same as that found for $Nb_8W_9O_{47}$ (1, 16). A characteristic feature of this structure is that the pentagonal tunnels are almost regular pentagons if they are occupied by M–O chains while unoccupied pentagonal tunnels appear much more distorted. The most significant difference of the $Nb_7W_{10}O_{47}$ structure to the previous models for $Nb_8W_9O_{47}$ is that the atomic positions

TABLE 3
Anisotropic Displacement Parameters (Å$\times 10^4$) for $Nb_7W_{10}O_{47}$

Atom	U^{11}	U^{22}	U^{33}	U^{23}	U^{13}	U^{12}
(Nb, W)(1)	87(2)	87(2)	60(2)	0	0	− 13(1)
(Nb, W)(3)	38(1)	62(1)	53(1)	1(1)	7(1)	3(1)
(Nb, W)(5)	52(1)	92(1)	63(1)	2(1)	− 2(1)	15(1)
W(6)	38(1)	57(1)	61(1)	− 3(1)	− 2(1)	2(1)
(Nb, W)(7)	76(1)	71(1)	84(1)	5(1)	1(1)	17(1)
(Nb, W)(8)	53(1)	51(1)	70(1)	4(1)	2(1)	1(1)
(Nb, W)(9)	48(2)	64(2)	66(2)	0(2)	2(2)	− 2(1)

Note. The anisotropic displacement factor exponent takes the form: $-2\pi^2[h^2a^2U^{11} + \cdots + 2hkabU^{12}]$.

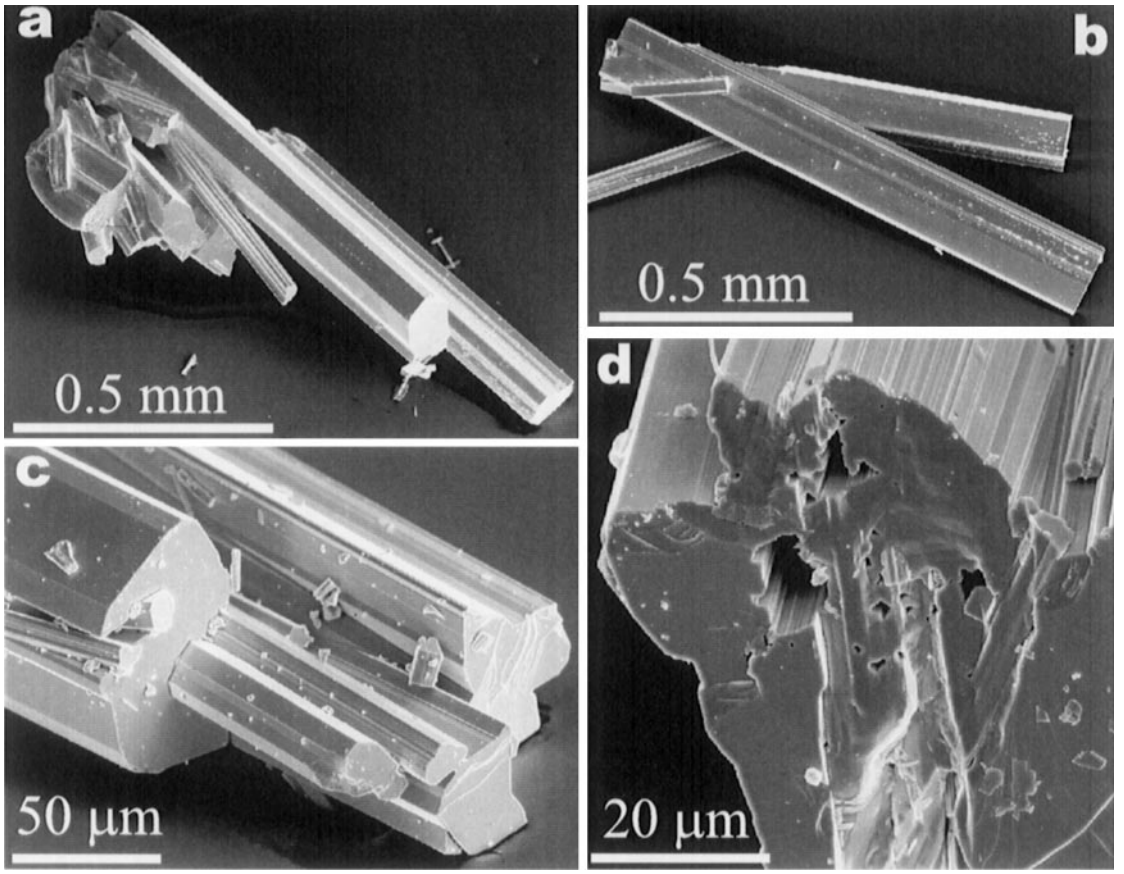

FIG. 1. SEM images of $Nb_7W_{10}O_{47}$: (a), (b) needles of different lengths, (c) bundle of needless in which several individuals are intergrown, and (d) end of a needle with channels running along the needle axis.

are considerably shifted out of the planes (001) and (002). This leads to a distortion of the polyhedra and to significantly different metal–oxygen distances in the direction of the *c* axis (Table 4). The short *M*–O distances range from 171.1 to 177.4 pm while the long distances range from 217.5 to 224 pm. The average difference between the *M*–O distances is about 44.7 pm with the maximal difference being 52.9 pm for Nb2B.

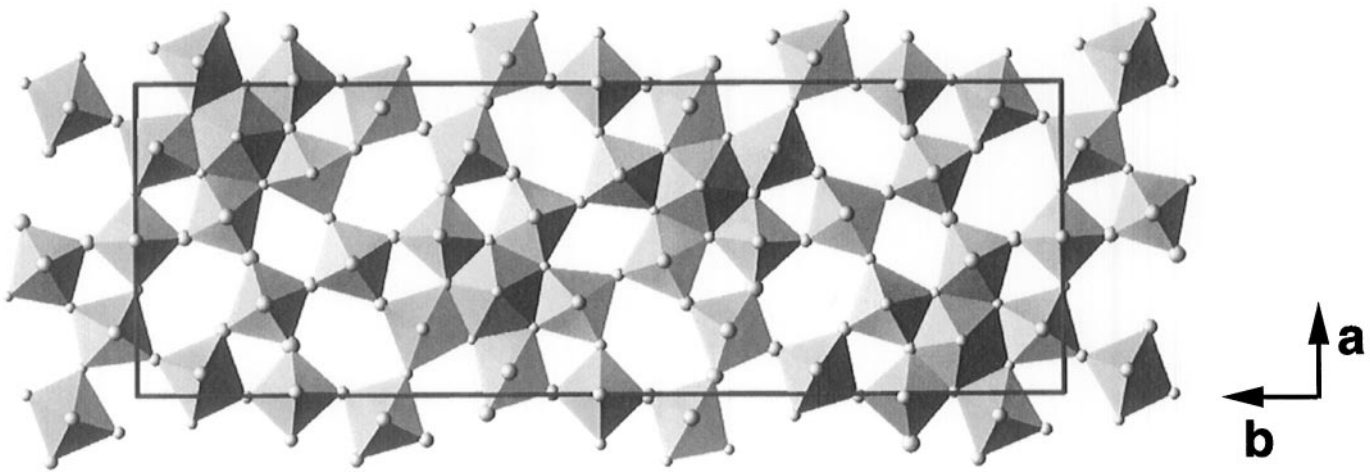

FIG. 2. Structure of $Nb_7W_{10}O_{47}$ projected along the *c* axis.

TABLE 4
Bond Lengths [pm] for $Nb_7W_{10}O_{47}$

(Nb, W)(1)–O(3)	174.5(6)	(Nb, W)(4A)–O(7)	176.0(4)	(Nb, W)(7)–O(6)	176.5(4)
–O(17)	191.3(5)	–O(23)	183.7(4)	–O(16)	181.4(4)
–O(17)	191.3(5)	–O(11)	188.3(5)	–O(11)	196.7(5)
–O(24)	195.8(4)	–O(15)	208.6(4)	–O(13)	199.9(4)
–O(24)	195.8(4)	–O(20)	209.5(4)	–O(23)	201.4(4)
–O(3)	220.4(6)	–O(7)	219.7(4)	–O(6)	218.5(5)
(Nb, W)(2A)–O(8)	176.1(4)	Nb(4B)–O(7)	175.5(5)	(Nb, W)(8)–O(4)	176.5(4)
–O(10)	187.5(5)	–O(23)	184.1(5)	–O(24)	185.1(5)
–O(22)	192.0(4)	–O(11)	186.9(5)	–O(22)	189.2(4)
–O(14)	203.1(4)	–O(15)	208.7(4)	–O(21)	201.3(4)
–O(21)	206.5(4)	–O(20)	210.1(4)	–O(12)	205.5(4)
–O(8)	218.9(4)	–O(7)	220.2(5)	–O(4)	218.6(4)
Nb(2B)–O(8)	171.1(8)	(Nb, W)(5)–O(5)	174.7(5)	(Nb, W)(9)–O(9)	177.4(3)
–O(10)	187.3(6)	–O(18)	191.8(5)	–O(12)	205.1(4)
–O(22)	190.0(6)	–O(25)	193.4(4)	–O(14)	206.2(4)
–O(14)	206.0(6)	–O(16)	197.1(4)	–O(15)	206.4(4)
–O(21)	206.9(6)	–O(10)	197.4(5)	–O(21)	213.0(4)
–O(8)	224.0(8)	–O(5)	220.3(5)	–O(20)	214.2(4)
(Nb, W)(3)–O(2)	175.5(4)	W(6)–O(1)	173.9(4)	–O(9)	217.5(3)
–O(18)	185.6(5)	–O(13)	180.0(4)		
–O(17)	186.3(5)	–O(25)	182.3(4)		
–O(20)	200.0(4)	–O(15)	198.7(4)		
–O(12)	204.1(4)	–O(14)	203.7(4)		
–O(2)	219.6(4)	–O(1)	221.4(4)		

This phenomenon has also been encountered in the other niobium tungsten oxides that contain pentagonal columns (PCs) as the main structural element. Nb_2WO_8 (22) as well as the quaternary phase $Na_7Nb_{15}W_{13}O_{80}$ (23) show similar distortions of the polyhedra in combination with alternating short and long M–O distances along the short crystallographic axis. The M–O distances are of comparable length in these structures. Nb_2WO_8 crystallizes in the $LiNb_6O_{15}F$ type (24). It is interesting to note that all atoms in $LiNb_6O_{15}F$ are located on the positions $x, y, 0$ and $x, y, 1/2$,

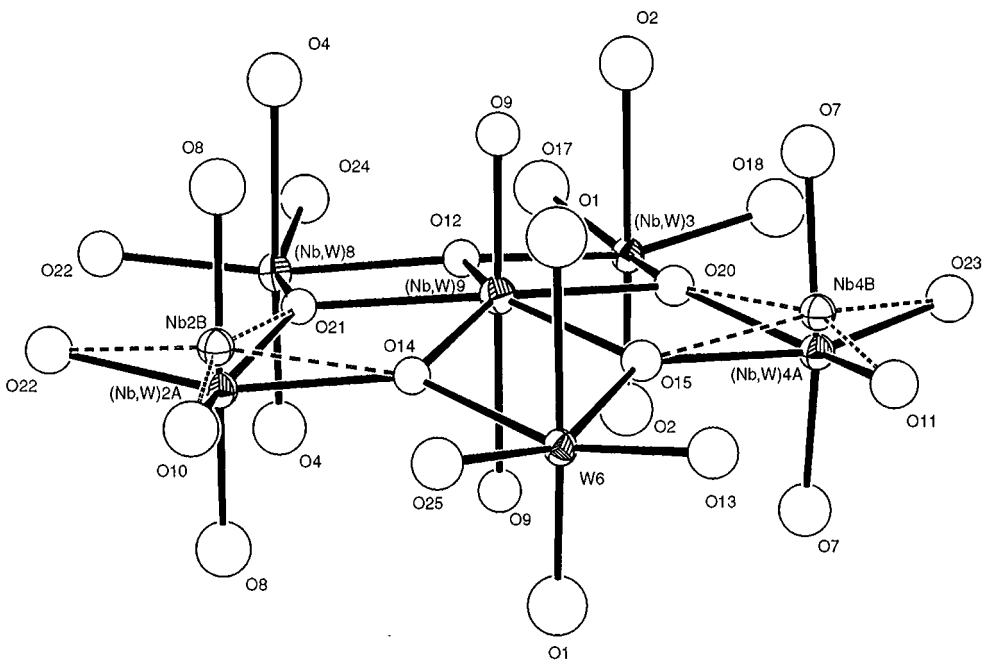

FIG. 3. View of a pentagonal column (PC) built up by five MO_6 octahedra surrounding a central MO_7 pentagonal bipyramid.

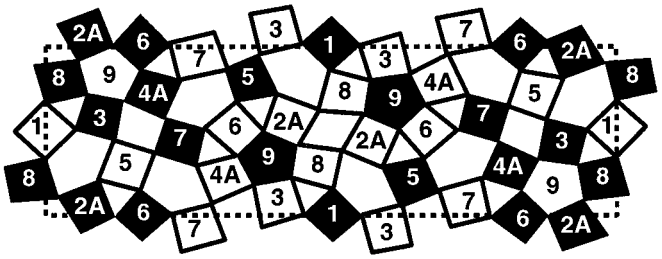

FIG. 4. Simplified structure model of $Nb_7W_{10}O_{47}$ (viewed along the *c* axis), qualitatively demonstrating the displacements of the cations along the *c* axis. The parameter *z* of cations inside filled polyhedra is $z > 0.5$; inside empty polyhedra $z < 0.5$. The numbers are those of the cations inside the corresponding polyhedra.

so that (001) and (002) indeed are mirror planes. The reduction of symmetry associated with the distortion of polyhedra in the PC seems to be a typical feature of niobium tungsten oxides. The inhomogeneous distribution of Nb and W atoms on the cation positions may contribute to this distortion.

The cations inside a PC are shifted out of the planes (001) and (002) in a characteristic way (Fig. 3): the displacement of the central cation inside the PC on the one hand and of the five cations in the surrounding octahedra on the other hand occur in opposite directions (Fig. 4; the scarcely occupied split positions Nb2B and Nb4B are not considered). A PC is connected via a square of octahedra (so-called diamond link (12)) to another one. In these PC pairs, both pentagonal bipyramidally coordinated cations have the same *z* coordinate. Two orientations of these PC pairs appear in the structure (Fig. 2) according to the symmetry of the space group, and the relative displacement of corresponding cations in *z* is therefore inverse.

The total composition of $Nb_{6.7}W_{10.3}O_{47}$ determined by subsequent refinement is in good agreement with the overall composition $Nb_7W_{10}O_{47}$ of the sample from which the crystal has been selected. As expected, large correlation matrix elements between the overall scale factor and the total amount of tungsten in the unit cell occured when the occupation ratios W/Nb on all metal atom positions were refined freely. Therefore, the metal atom site *M*6 which appeared to have the highest W/Nb ratio was assumed to be occupied exclusively by tungsten atoms. In the structure models of $Nb_7W_{10}O_{47}$ and of $Nb_8W_9O_{47}$ (1), *M*6 is occupied by W atoms only while there is a large surplus of Nb in the pentagonal bipyramidal coordinated site *M*9.

The investigation of other crystals of less quality, namely those with a composition close to $Nb_8W_9O_{49}$, led to similar strucural models (25). However, all results strongly suggest that the crystal structure is essentially the same for all phases $(Nb, W)_{17}O_{47}$, differing only in the actual occupation ratios of the cation sites with niobium and tungsten atoms.

ACKNOWLEDGMENT

We thank Peter Wägli for performing the SEM investigation.

REFERENCES

1. A. W. Sleight, *Acta Chem. Scand.* **20,** 1102 (1966).
2. A. Magnéli, *Arkiv Kemi.* **24,** 213 (1949).
3. R. S. Roth and J. L. Waring, *J. Res. Natl. Bur. Stand. A* **70,** 281 (1966).
4. M. W. Viccary and R. J. D. Tilley, *J. Solid State Chem.* **104,** 131 (1993)
5. F. Krumeich, A. Hussain, C. Bartsch, and R. Gruehn, *Z. Anorg. Allg. Chem.* **621,** 799 (1995).
6. F. Krumeich, G. Liedtke, and W. Mader, *Z. Anorg. Allg. Chem.* **623,** 990 (1997).
7. F. Krumeich and T. Geipel, *J. Solid State Chem.* **124,** 58 (1996).
8. S. M. Montemayor, A. A. Mendez, A. Martinez de la Cruz, A. F. Fuentes, and L. M. Torres-Martinez, *Chem. Matter.* **8,** 2777 (1998).
9. M. Lundberg and B.-O. Marinder, *J. Solid State Chem.* **84,** 23 (1990).
10. M. Lundberg and M. Sundberg, *J. Less-Common Met.* **137,** 163 (1988).
11. M. Lundberg, *Chem Commun. Univ. Stockholm* **XII** (1971).
12. M. Lundberg, M. Sundberg, and A. Magnéli, *J. Solid State Chem.* **44,** 32 (1982).
13. M. Iijima and J. G. Allpress, *Acta Crystallogr. Sect. A* **30,** 22 (1974).
14. S. Horiuchi, K. Muramatsu, and Y. Matsui, *Acta Crystallogr. Sect. A* **34,** 939 (1978).
15. L. Eyring, *in* "High-Resolution Transmission Electron Microscopy and Associated Techniques" (P. Buseck, J. Cowley, and L. Eyring, Eds.), p. 378. Oxford University Press, New York/Oxford, 1994.
16. D. C. Craig and N. C. Stephenson, *Acta Crystallogr. Sect. B* **25,** 2071 (1969).
17. "SAINT," Version 4.05, Siemens Analytical X-ray Instruments, Madison, Wisconsin.
18. "SHELXTL" program package, Version 5.1, Bruker AXS Inc., Madison, Wisconsin.
19. "SADABS," G. Sheldrick, Göttingen, 1997.
20. "X-SHAPE," Version 1.01, Stoe and Cie GmbH, Darmstadt, 1996.
21. G. Heurung and R. Gruehn, *J. Less-Common Met.* **76,** 17 (1980).
22. M. Lundberg, *Acta Chem. Scand.* **26,** 2932 (1972).
23. B. -O. Marinder and M. Sundberg, *Acta Crystallogr. Sect. C* **40,** 1303 (1984).
24. M. Lundberg, *Acta Chem. Scand.* **19,** 2274 (1965).
25. M. Wörle and F. Krumeich, unpublished results.